RSC Advances

PAPER

View Article Online
View Journal | View Issue

Cite this: *RSC Adv.*, 2016, **6**, 66579

Thermogravimetric study of sequential carbonation and decarbonation processes over Na_2ZrO_3 at low temperatures (30–80 °C): relative humidity effect

J. Arturo Mendoza-Nieto* and Heriberto Pfeiffer

In the present work, Na_2ZrO_3 was synthetized *via* a solid-state reaction and characterized by powder X-ray diffraction and N_2 physisorption techniques, where desired structural and microstructural characteristics were confirmed. Then, the ceramic material was tested dynamically and isothermally in a low temperature range (30–80 °C) for carbonation and decarbonation processes using relative humidity (RH) values between 0 and 80%. Thermogravimetric results indicate that humidity has a positive influence over the carbonation process, thus the amount of CO_2 captured increases as a function of relative humidity. When high values of humidity (70 and 80%) were used, the increase in sample weight was higher than the theoretical amount of 57.2 wt% expected in wet conditions. This result was attributed to the formation of $NaHCO_3$ with a mesoporous microstructure. Then, the relative humidity effect was studied during the decarbonation stage as a sequential step after the carbonation process, using a N_2 flow. Infrared spectroscopy and thermogravimetric results showed that $NaHCO_3$ decomposition took place in this process. At low RH values, 0 and 20%, $NaHCO_3$ is decomposed in Na_2O and Na_2CO_3; whereas, when RH was increased between 40 and 80%, only the presence of Na_2CO_3 was observed. This result indicates that at high humidity conditions the Na_2O formation is avoided. Thermal curves show that Na_2CO_3 decomposition presented a maximum efficiency at 40% of RH, which seems to be the optimal condition for the decarbonation step. Finally, sequential carbonation–decarbonation tests were performed with sodium zirconate samples. Infrared and thermal analyses confirm that it is possible to accomplish successively at least eight cycles of carbonation and decarbonation steps and to obtain high $NaHCO_3$ and Na_2CO_3 regenerations.

Received 14th May 2016
Accepted 7th July 2016

DOI: 10.1039/c6ra12533f

www.rsc.org/advances

1. Introduction

Nowadays, greenhouse gas (GHG) emissions, such as methane (CH_4), nitrous oxide (N_2O) and carbon dioxide (CO_2), are responsible for several ambient damages, including climate change and global warming. Among GHG, CO_2 emissions are the main contaminations, contributing to almost 60% of the enhanced greenhouse effect each year.[1] In order to diminish carbon dioxide effects, many technologies have been proposed for CO_2 capture and storage (CCS).[2,3] For this purpose, a wide variety of materials have been used as chemical sorbents, *e.g.* zeolites,[4–6] Metal–Organic Frameworks (MOFs),[7,8] amine-modified mesoporous materials (SBA-15, MCM-41 and HMS),[6,9,10] alkali (Li, Na and K)[11–14] and alkaline-earth (Be, Mg and Ca)[15–17] metal-based ceramics.

Among alkali ceramics, sodium zirconate (Na_2ZrO_3) is a ceramic material that has been synthetized, characterized and used as a catalytic material or chemical sorbent for different reactions due to good physicochemical properties, high surface basicity, mechanical strength, thermal stability until 900 °C and high regeneration ability, *e.g.* biodiesel production by soybean oil transesterification,[18] hydrogen production through methane reforming,[19] carbon monoxide (CO) oxidation[20] and carbon dioxide capture and storage at $T > 500$ °C, showing high capacity in the last process.[21–25]

One goal in CCS is to increase the amount of CO_2 captured during a carbonation process. In this line, it has been proposed the incorporation of water vapor into the reaction system as a promissory condition for enhancing the chemisorption of carbon dioxide. Thus, it has been already studied the chemisorption ability of Na_2ZrO_3 in absence[24,26,27] and presence[28,29] of water vapor. Results showed that in dry conditions sodium zirconate is able to capture between 10 and 24 wt% of CO_2 in a high temperature range (500–850 °C), obtaining the highest capture at around 550 °C. On the other hand, when water vapor was added, the chemisorption process took place at much lower temperature, between 40 and 70 °C, obtaining higher amounts of CO_2 captured (25–35 wt%) than in dry conditions at similar thermal conditions, as it was described above. The reaction mechanism for the Na_2ZrO_3–CO_2–H_2O system was presented by Santillán-Reyes G. *et al.*[28] as follow: Na_2ZrO_3 ceramic reacts with

Instituto de Investigaciones en Materiales, Universidad Nacional Autónoma de México, Ciudad Universitaria, Circuito exterior s/n, Del. Coyoacán, CP 04510, México DF, Mexico. E-mail: amendozan@comunidad.unam.mx; Fax: +52 55 5616 1371; Tel: +52 55 5622 4627

water vapor to produce in the beginning of the process hydroxyl species at the particle surfaces and then absorbs 2 mol of CO_2 and 1 mol of H_2O to eventually form 2 mol of $NaHCO_3$ and ZrO_2. This mechanism clearly show the benefits of using wet atmosphere during CO_2 chemisorption, allowing capture higher amount of carbon dioxide than in dry conditions, where only 1 mol of CO_2 can be captured as a result of the chemisorption process. In this line, Na_2ZrO_3 can be proposed as a solid adsorbent at low temperatures in a post-combustion capture technologies,[30] where wet environments are due to the water vapor presence as a combustion product.[31]

Also, Na_2ZrO_3 regeneration ability in sequential CO_2 carbonation and decarbonation processes has been studied at high temperature range.[22,32,33] Results showed clearly that sodium zirconate regeneration is feasible, after several sequential steps of CO_2 chemisorption and desorption in a high temperature range between 500 and 800 °C, due to high thermal stability. However, up to now Na_2ZrO_3 regeneration ability for sequential CO_2 carbonation and decarbonation processes have not been deeply studied when water vapor is added in the system at low temperatures. Therefore, the aim of this work was to test the carbon dioxide absorption and desorption ability of Na_2ZrO_3 and then elucidate if relative humidity (RH) has a significant influences over carbonation and decarbonation processes in a low temperature range (30–80 °C).

2. Experimental section

2.1 Synthesis and characterization

Sodium zirconate (Na_2ZrO_3) was synthesized by well-known procedure of solid state reaction, previously reported.[24,27,34] Sodium carbonate (Na_2CO_3, Aldrich) and zirconium oxide (ZrO_2, Aldrich) were used as reagents. During the synthesis, 10 wt% of Na_2CO_3 excess was considered, due to the high tendency of Na to sublimate at temperatures higher than 800 °C. Thus, the Na_2CO_3 : ZrO_2 molar ratio employed was 1.1 : 1.0. Then, precursor salts were mechanically mixed and calcined in air atmosphere at 900 °C for 12 h.

The ceramic obtained was characterized structurally and microstructurally by powder X-ray diffraction (XRD) and nitrogen adsorption-desorption analyses. XRD pattern was recorded in the $10° \leq 2\Theta \leq 70°$ range, using a goniometer speed of $1°(2\Theta)\ min^{-1}$, with a diffractometer Siemens D5000 coupled to a cobalt anode ($\lambda = 1.789$ Å) X-ray tube. Once the Na_2ZrO_3 crystalline structure was confirmed, nitrogen adsorption-desorption isotherms were measured with a Bel-Japan Minisorp II equipment at 77 K using a multipoint technique. Prior to the physisorption experiment, the ceramic sample was degassed ($p < 10^{-1}$ Pa) at room temperature for 12 h in vacuum. Finally, specific surface area (S_{BET}) was calculated according to the BET method.

2.2 Thermal analyses

Dynamic and isothermal tests for carbonation and decarbonation processes were performed using a humidity-controlled thermobalance (TA Instruments, model Q5000SA) at different temperatures (30–80 °C) and relative humidities (0–80%). All these experiments were performed using 40 mg of sample, distilled water into the humidity chamber and two different carrier gases: carbon dioxide (CO_2, Praxair grade 3.0) for carbonation step and nitrogen (N_2, Praxair grade 4.8) during decarbonation process. The total gas flow rate used in the experiments was 100 mL min^{-1} and the relative humidity (RH) percentages were automatically controlled by the Q5000SA equipment.

Thermal analyses were performed in three sections. In the first part, a set of Na_2ZrO_3 samples were heat-treated dynamically in a CO_2 gas flow, with a heating rate of 0.5 °C min^{-1} from 30 to 80 °C maintaining RH constant at 0, 10, 20, 40, 60 and 80%. In the second experimental section, Na_2ZrO_3 samples were isothermically carbonated at 80 °C and 80% of RH during 2 h using a CO_2 flow, continuing with a decarbonation step under N_2 as a carrier gas and setting RH at different values (0, 20, 40, 60 and 80%) during 4 h. Finally, in the third part of the experimentation, carbonation and decarbonation steps were undertaken successively at 80 °C using the best conditions of RH obtained for each step: 80% of RH for carbonation step and 40% of RH for decarbonation step.

Afterwards, the products obtained from dynamic and isothermal tests were characterized by attenuated total reflection infrared spectroscopy (ATR-FTIR) and thermogravimetric analysis (TGA). For ATR-FTIR spectroscopy an Alpha-Platinum spectrometer from Bruker was used, whereas TG measurements were performed using 10 mg of sample under nitrogen atmosphere in a Q500HR equipment from TA Instruments at a heating rate of 10 °C min^{-1} from 30 to 800 °C.

3. Results and discussion

3.1 Sodium zirconate characterization

Powder X-ray diffraction pattern of sodium zirconate is shown in Fig. 1A. The XRD pattern exhibits well-resolved signals which were all fitted to the JCPDS-ICDD card 35-0770, corresponding to monoclinic crystal structure of sodium zirconate. The above result shows that the ceramic obtained is conformed only by the desired crystalline phase without impurities. In Fig. 1B, nitrogen adsorption–desorption isotherm for Na_2ZrO_3 sample is shown. According to IUPAC classification, the ceramic material presents a type II isotherm related to nonporous materials.[35] In this material, no hysteresis loop was observed in the isotherm shape. Additionally, specific surface area (S_{BET}) was determined from N_2 adsorption curve using the BET method. The S_{BET} value obtained was equal to 3.0 $m^2\ g^{-1}$, which is in line with the method of solid-state used for the Na_2ZrO_3 synthesis. Also, the above nitrogen physisorption results obtained for sodium zirconate are well in agreement with previous publications.[26,28]

3.2 Thermal analyses

3.2.1 Dynamic tests. Once Na_2ZrO_3 was characterized, the ceramic was thermally treated from 30 to 80 °C under different values of RH between 0 and 80%, into a thermobalance. In all

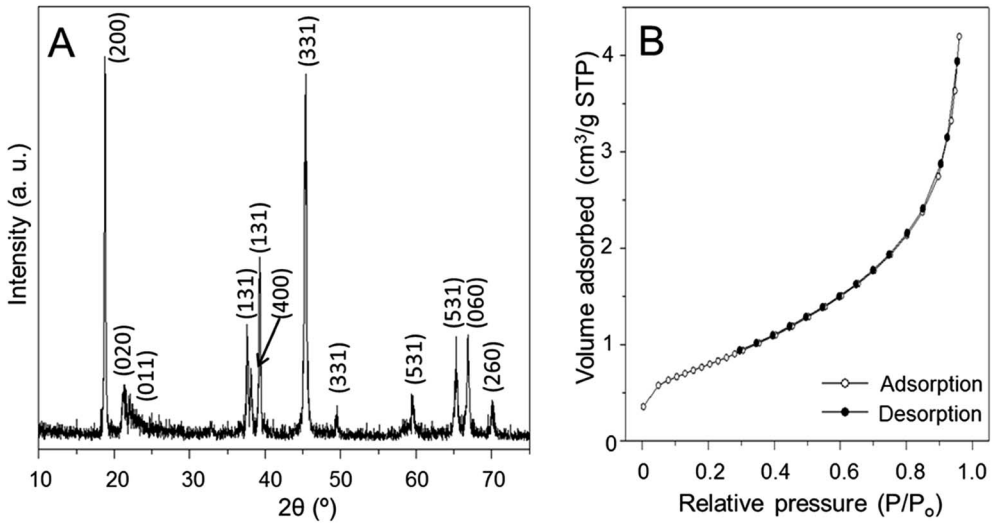

Fig. 1 XRD pattern (A) and N_2 adsorption–desorption isotherm (B) of Na_2ZrO_3.

thermograms in Fig. 2A, it was observed a weight increase as function of temperature and RH percentage. In dry conditions (0% RH), sodium zirconate was able to chemisorbed 20.5 wt% of CO_2. Then, the weight increase observed in this case is due to the sodium carbonate (Na_2CO_3) formation, as it was reported previously.[24] This amount is near to the theoretical amount of CO_2 that can be chemisorbed in dry conditions (23.8 wt%), according to reaction (1).

$$Na_2ZrO_{3(s)} + CO_{2(g)} \rightarrow Na_2CO_{3(s)} + ZrO_{2(s)} \quad (1)$$

When a wet condition was employed, a higher weight increase was observed. This behavior may be due to the sodium bicarbonate ($NaHCO_3$) formation, during the hydration–carbonation processes in presence of water vapor and CO_2, as reaction (2) shows.

$$Na_2ZrO_{3(s)} + 2CO_{2(g)} + H_2O_{(v)} \rightarrow 2NaHCO_{3(s)} + ZrO_{2(s)} \quad (2)$$

It has been described in the literature[15,28,36–38] that the addition of water vapor significantly improves the amount of CO_2 chemisorbed on different ceramic materials. Thus, in this case, if water molecules react with sodium zirconate, superficially, Na–OH species should be produced. Then, the activated surface must be more reactive for CO_2 chemisorption. Therefore, Na_2ZrO_3 may have reacted with CO_2 because of a hydroxylated surface, producing sodium bicarbonate.

In Fig. 2A it can be seen that the addition of water vapor into the reaction system significantly improves the total weight

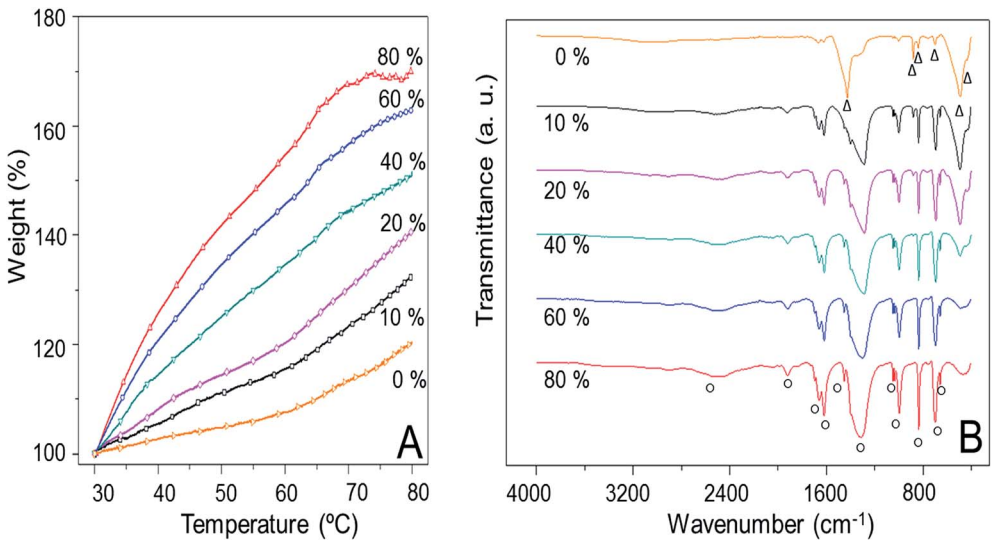

Fig. 2 TG (A) and ATR-FTIR spectra (B) of Na_2ZrO_3 samples tested dynamically in CO_2 chemisorption with 0, 10, 20, 40, 60 and 80% of RH. (△) Na_2CO_3 and (○) $NaHCO_3$ vibration bands.

increment. In fact, using low values of relative humidity, *e.g.* 10%, it was possible to gain 32.5 wt%. This amount is 36.5% higher than the theoretical amount of CO_2 chemisorbed in dry conditions, according to reaction (1). As the percentage of RH increases in Fig. 2A, the weight of the sample increases too. At this point, it must be pointed out that the theoretical maximum amount of CO_2 that can be chemisorbed over sodium zirconate sample is 57.2 wt% in wet conditions, according to reaction (2). However, the dynamic profiles of the samples tested at 60 and 80% of RH importantly reached higher percentages: 62.8 and 69.0 wt%, respectively. According to Martínez-dlCruz *et al.*,[27] the above result could be associated to a mesoporous $NaHCO_3$ external shell formation as a consequence of the CO_2 chemisorption over the ceramic surface. Therefore, the presence of this type of pores in the external shell allowed CO_2 diffusion chemisorption. In addition, the exceeded weight increment (11.8 wt%), which could be associated to a water adsorption on the surface and porosity produced.

All the products of dynamic tests were characterized *via* ATR-FTIR in order to determinate the composition in the sample. The corresponding spectra are shown in Fig. 2B. In dry conditions, as expected, the sample is composed by Na_2CO_3, according to the vibration bands located at 420, 490, 697, 840, 880 and 1402 cm^{-1} in the FTIR spectrum. The spectra of samples treated with water vapor addition (10–80% RH) present vibration bands at 660, 692, 836, 998, 1037, 1050, 1300, 1454, 1623, 1662, 1910 and 2508 cm^{-1}. All these bands fitted well with the $NaHCO_3$ FTIR spectrum.[28,39] Independently of RH used during the dynamic tests, the presence of sodium bicarbonate was established. Also, it can be observed other bands located at 420, 490, 840 and 1402 cm^{-1} in the samples spectra of the products treated at 10, 20 and 40% of RH. These vibration bands correspond to sodium carbonate FTIR spectrum.[28] In Fig. 2B, an increase in the intensity of the $NaHCO_3$ vibration bands and a decrease in the Na_2CO_3 bands were observed when the RH percentage employed increases from 10 to 80%. This result shows that the formation of $NaHCO_3$ is benefited at high relative humidity values. Also, the above result indicates that a low RH values (≤40%), the reactions (1) and (2) proceed at the same time due to the low amount of water vapor into the reaction system, producing the formation of two carbonated compounds: Na_2CO_3 and $NaHCO_3$; whereas at RH percentages higher than 40%, the bicarbonate sodium is the only carbonated compound present in the sample.

With the aim for determining if a $NaHCO_3$ porous core shell was formed in the samples humidity-treated at high values of RH, the sample carbonated dynamically at 80% of RH was characterized *via* nitrogen adsorption–desorption (Fig. 3). For comparison purposes, the isotherm of the original sample was presented as well. Both isotherms present a type II isotherm with no hysteresis loop evident. The sample humidity-treated presented a S_{BET} value equal to 11.7 $m^2\ g^{-1}$, that is almost four times bigger than the superficial area obtained for the original sample (3.0 $m^2\ g^{-1}$). This result confirms the idea of the porous or somehow texturized core shell formation due to the carbonation species chemisorbed over the sodium zirconate.

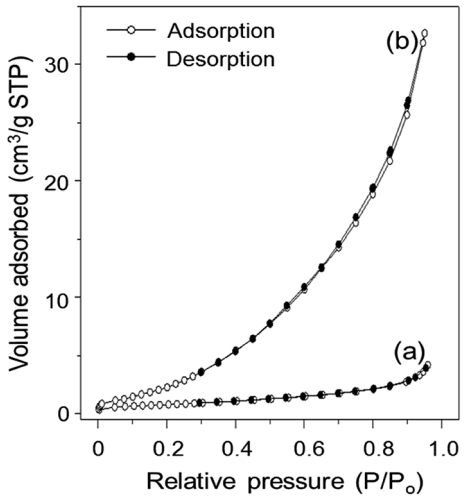

Fig. 3 N_2 adsorption–desorption isotherms of (a) original sodium zirconate and (b) sample treated dynamically at 80% of RH in a CO_2 flow.

Then, the products tested in the presences of water vapor at different RH values, were analyzed also by thermogravimetric analysis in order to determinate the decomposition temperature of carbonated compounds present in the samples. The thermogravimetric (TG) and derivate thermogravimetric (DTG) curves are shown in Fig. 4. The decomposition profiles, as expected, presented a decrease in the sample weight at different temperatures. The first weight lost, near to 100 °C in all samples, is the most important weight decrease. The process that takes place at this temperature is the decomposition of $NaHCO_3$ in Na_2CO_3, as reaction (3) shows. As it can be seen in Fig. 4A, the lost weight increases when the relative humidity increases from 10 to 80%.

$$2NaHCO_{3(s)} \rightarrow Na_2CO_{3(s)} + H_2O_{(v)} + CO_{2(g)} \quad (3)$$

The theoretical percentage that the sample can lose is 21.3 wt% according to reaction (3). The sample tested at 40% of RH shows almost the theoretical amount (20.6 wt%); however, the samples humidity-treated at 60 and 80% of RH, presented higher weight lost: 23.5 and 24.0 wt% respectively, at temperatures ≤200 °C. The above result indicates that in the samples tested at 60 and 80% of RH presented a partial hydration process. This result is in agreement with the observation made it at dynamic tests, where it was propose that a carbonated core shell with mesopores was formed during the capture of CO_2 in wet conditions (RH ≥ 60%), allowing the capture of CO_2, forming sodium bicarbonate, and the H_2O adsorption.

Additionally, between 230 and 350 °C, the profiles of the samples treated at low RH values (10 and 20%) presented a decrease of 6.0 and 4.0 wt%, respectively. The weight lost in these samples can be attributed to the superficial dehydroxylation process,[28] indicating a non-complete carbonation process. The rest of the samples do not present any weight decrease in this range of temperature. Finally, at temperatures

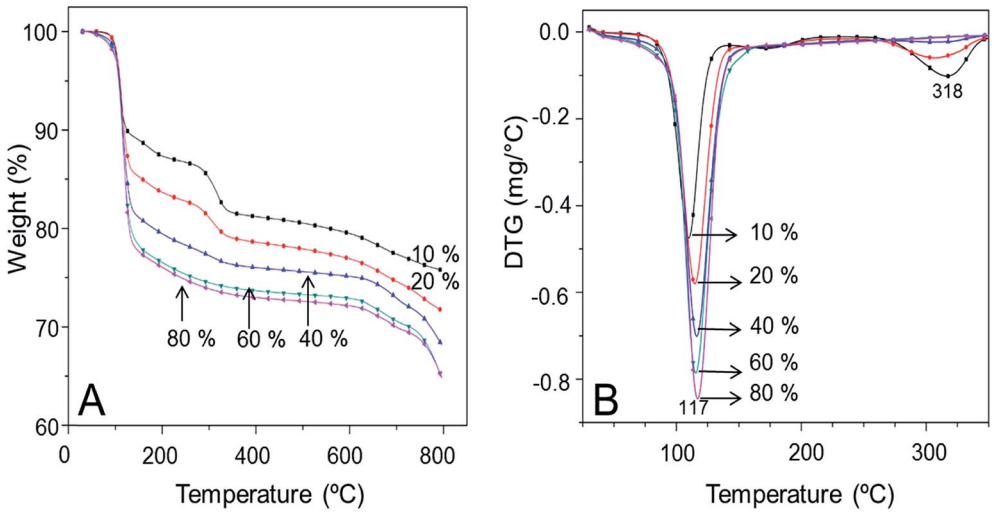

Fig. 4 TG (A) and DTG (B) curves for products obtained in dynamic tests.

higher than 600 °C all the samples began to lose weight due to decarbonation process in the Na_2ZrO_3 particles.

DTG curves obtained from TGA profiles are presented in Fig. 4B. These analyses allow us to determinate the temperature that the processes described above occur. All samples present an endothermic peak located between 85 and 145 °C with maximum in 117 °C, which is related to the $NaHCO_3$ decomposition under nitrogen flow. This result shows that the presence of sodium bicarbonate increases as function of RH percentage. Thus, the highest amount of $NaHCO_3$ was formed when 80% of RH was employed and as expected this sample presented the larger endothermic peak at low temperature (≤150 °C) among all samples decomposed.[40] Only the curves of samples treated at 10 and 20% of RH, presented a second distribution with maximum at 318 °C that was ascribed to the superficial dehydroxylation and Na_2CO_3 decomposition.

3.2.2 Carbonation stage. Once optimal conditions for carbonation process were determined, a Na_2ZrO_3 sample was carbonated isothermically during 2 h using the best conditions found in the dynamic tests (80 °C and 80% of RH) in a CO_2 flow. Thermogravimetric analyses are shown in Fig. 5. As it can be seen, an increased weight as a function of time was registered in Fig. 5A. The maximum amount of CO_2 captured was 69.0 wt%, that corresponds to CO_2 capture of 13.0 mmol per gram of ceramic material if a total formation to $NaHCO_3$ is assumed, where the rest 11.8 wt% of the total weight gained must correspond to adsorbed water. This hypothesis was confirmed after the product ATR-FTIR characterization, where sodium bicarbonate vibration bands were the only signals present (spectrum not shown). The CO_2 amount chemisorbed in this stage represents a high value in comparison with other works where the maximum capture over Na_2ZrO_3 was obtained between 10 and 25.0 wt% at T > 550 °C.[24,26,27] This result clearly show the advantages to use water vapor into the system during the carbonation step: increases in almost three times the CO_2 capture and also decreases drastically the temperature (80 °C)

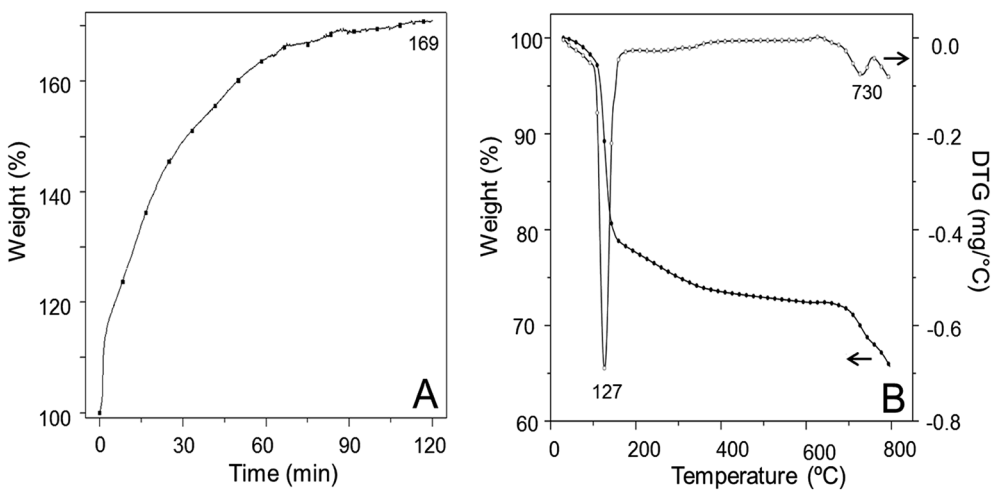

Fig. 5 Carbonation isotherm (A) and thermogravimetric analyses (B) of Na_2ZrO_3 sample tested under CO_2 flow at 80 °C and 80% of RH.

where the chemisorption process took place. Also, the CO_2 capture of 69.0 wt% is higher in comparison with other works where alkali-based ceramics[28,31,41,42] were used in atmosphere of water vapor at low temperature range (30–80 °C). This result can be related to the S_{BET} present in the sample prepared that is at least two or three times higher than the superficial areas reported for those ceramics, beneficiating the superficial phenomena and the $NaHCO_3$ mesopore core shell formation that occur during the CO_2 chemisorption at low temperatures.

After, the isothermal product was characterized by TG and DTG analyses (Fig. 5B), the decomposition profile presented a similar behavior than that previously observed in the sample treated dynamically at 80% of RH (Fig. 4). The decomposition curve shows a main decrease between 100 and 135 °C, related with the decomposition of $NaHCO_3$ to Na_2CO_3. According to DTG result this process took place at 127 °C. The temperature obtained in this case is higher than those obtained in the DTG curve of the sample treated dynamically at 80% RH (117 °C, Fig. 4B). This can be due to the differences in the experiments conditions. In dynamic test, the temperature increases from 30 to 80 °C during the experiment, whereas in the isothermal test, the experimental conditions were maintained at 80 °C during 2 h. Finally, the second weight decrease in TGA profile began at 730 °C according to DTG curve. This weight loss was attributed to decarbonation process.

3.2.3 Decarbonation stage. After the carbonation process, a decarbonation step was undertaken in a dynamic test with values of RH between 0 and 80%, under a N_2 flow. Fig. 6 presents the results of the isotherm at 80 °C of these two successively steps. The aim of this experiment was to determinate the effect of relative humidity over decarbonation process. The isotherm shows that in the first step the carbonation process at 80% of RH took place after 2 h. Immediately, the sample was exposed in a N_2 flow with 0% of RH and a decrease of 14 wt% was registered. Later, between 5 and 70% of RH, a continuous weight lost was observed until 42.8 wt%. The above weight decrease can be due to $NaHCO_3$ decomposition (see reaction (3)). Then, when the RH value was higher than 70% a weight increase of 4.0 wt% was observed, probably due to some water condensation over the ceramic surface as a result of the high relative humidity.

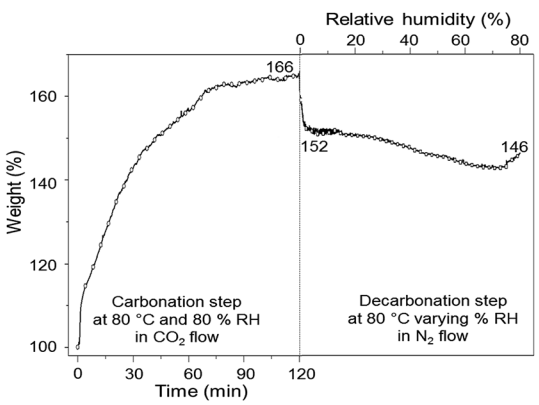

Fig. 6 Carbonation–decarbonation isotherm at 80 °C.

In order to deeply understand the phenomena occurring during the decomposition stage, a serial of experiments at 80 °C with values of RH equal to 0, 20, 40, 60 and 80% were undertaken during 4 h, maintaining constant the conditions of 80 °C and 80% of RH in the previous carbonation stage. After these tests, the products were collected and then analyzed *via* ATR-FTIR technique (Fig. 7), where some differences in the spectra were observed. As it can be seen, at low RH values (0 and 20%), the presence of sodium oxide and some traces of sodium carbonate were detected. The vibration bands located at 704, 762, 880, 990, 1465 and 1621 cm^{-1} were fitted with the Na_2O FTIR spectrum, whereas the bands observed at 430, 500, 840, 1360 and 1410 cm^{-1} were associated to Na_2CO_3 spectrum.[28] The Na_2CO_3 and Na_2O formation were due to the sequential $NaHCO_3$ and Na_2CO_3 decompositions under nitrogen flow, according to reactions (3) and (4). However, when CO_2 was desorbed during the decarbonation step, sodium atoms as Na_2O remain over the Na_2ZrO_3 particle surfaces. As the temperature and relative humidity are low, sodium atoms seems not to be kinetically able to be reincorporated in the sodium zirconate crystalline structure.[43]

$$Na_2CO_{3(s)} \rightarrow Na_2O_{(s)} + CO_{2(g)} \quad (4)$$

On the other case, when RH percentage was between 40 and 80%, only the presence of sodium carbonate was observed and additional vibration bands for sodium carbonate compound were observed at 618, 671, 697, 1049, 1647 and 1732 cm^{-1}. The Na_2O vibration bands were not detected anymore. This result indicates that $NaHCO_3$ was only decomposed in Na_2CO_3 in humid conditions. It seems that water vapor presence inhibits the sodium carbonate decomposition in sodium oxide. The spectra of humidity-treated samples at high RH percentage show a decrease of sodium carbonate in the sample when the RH value increases. Also in those spectra, an additional vibration band was observed at 3300 cm^{-1}, related to adsorbed water.

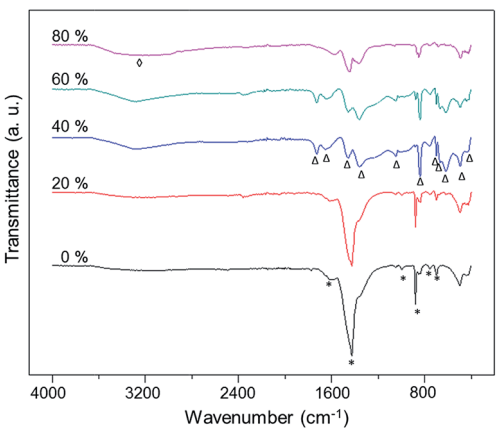

Fig. 7 ATR-FTIR spectra of Na_2ZrO_3 samples carbonated at 80 °C and 80% of RH and then decarbonated at 0, 20, 40, 60 and 80% of RH. (◇) OH, (*) Na_2O and (△) Na_2CO_3 vibration bands.

Carbonation–decarbonation products were characterized by TG and DTG analyses (Fig. 8). All the decomposition profiles presented two weight loss temperature ranges; $T < 200$ °C and $T > 650$ °C (Fig. 8A). Sample weight decrease as function of RH percentage was observed, thus the sample humidity-treated at 80% presented the highest weight lost among all the samples tested. Also, this sample was the only sample that presented a different behavior at low temperature range where a weight lost was observed around 90 °C, whereas the rest of the samples presented the weight lost at 115 °C, according to DTG curves (Fig. 8B). This variation is associated to the decomposition of Na_2O at low values of RH (10 and 20%), whereas at higher relative humidity percentages is related to the Na_2CO_3 decomposition. As it can be seen in DTG curves, the best sodium carbonate decomposition was presented at 40% of RH, which seems to be the optimal condition for decarbonation. When higher RH values than 40% of RH were used, a decrease in the amount of Na_2CO_3 decomposed was observed. In fact, sample humidity-treated at 80% of RH is the unique that presented two signals in DTG curve, that can be associated the first one to sodium carbonate decomposition at 115 °C and the second signal at 90 °C can be ascribed to water evaporation process. Finally, the second weight decrease in TGA profile (Fig. 8A) took place at around 720 °C. This weight loss was attributed to decarbonation process in the Na_2ZrO_3 particles.

3.2.4 Sequential carbonation and decarbonation stages. In this section, carbonation and decarbonation tests were sequentially performed in different stages labeled as half-stages and complete stages. Half-stages (0.5, 1.5 and 2.5) mean that a carbonation process was the last procedure taking place; whereas complete stages (1.0 and 2.0) show that the decarbonation process was carried at the end of the experimentation. Thus, in the stage 0.5, only the CO_2 chemisorption process was realized at 80 °C and 80% of RH for 2 h; whereas in the stage 1.0 a previous carbonation process took place in the same conditions described for the stage 0.5, followed by a decarbonation step at 80 °C and 40% of RH during 4 h. Then, carbonation and decarbonation processes were performed successively until five steps (3 carbonations and 2 decarbonations) were accomplished for the sample treated in the stage 2.5, using the conditions described above for carbonation and decarbonation steps.

In the TG profiles for the samples treated in the different stages can be seen that in all carbonation end-stages (0.5, 1.5 and 2.5), high amount of CO_2 and water were captured (between 65 and 69 wt%, data not shown) at 80% of RH, whereas in decarbonation end-stages (1.0 and 2.0), in all cases a decrease in weight between 15 and 20 wt% was observed as consequence of $NaHCO_3$ decomposition in sodium carbonate at 40% of RH. These results show that it was possible to capture high amounts of CO_2 and then desorb it in sequential carbonation–decarbonation stages at 80 °C. After that, all products obtained were collected and then characterized *via* ATR-FTIR and thermogravimetric analyses.

Fig. 9 shows the ATR-FTIR results for different carbonation–decarbonation stages. As expected, the sample tested only in carbonation step (stage 0.5), present vibration bands related to the presence of $NaHCO_3$ (vibration bands assigned in Fig. 2B). When the sample was tested successively in carbonation–decarbonation processes (stage 1.0), a different spectrum was observed. In this case, the vibration bands of Na_2CO_3 and –OH groups were detected in the sample. The above results confirm that after a carbonation process at 80% of RH, it is possible that a decarbonation step takes place when the sample is exposed in a nitrogen flow with the optimal RH of 40%. Then, when sample was exposed to the successively carbonation–decarbonation–carbonation steps (stage 1.5), in the spectrum were detected only vibration bands of $NaHCO_3$, confirming that high regeneration of sodium bicarbonate was accomplished. It seems that the presence of Na_2CO_3 on surface after a decarbonation step was beneficial for a second carbonation step, due that CO_2 capture can continue over this core shell of sodium carbonate and form again a core shell of $NaHCO_3$.

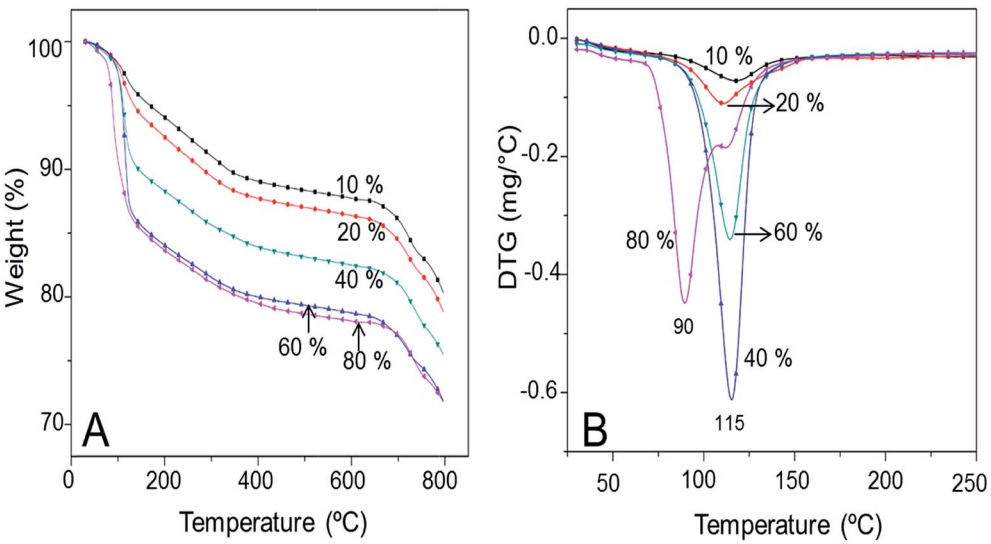

Fig. 8 TG (A) and DTG (B) curves of Na_2ZrO_3 samples carbonated at 80 °C and 80% of RH and then decarbonated at 0, 20, 40, 60 and 80%.

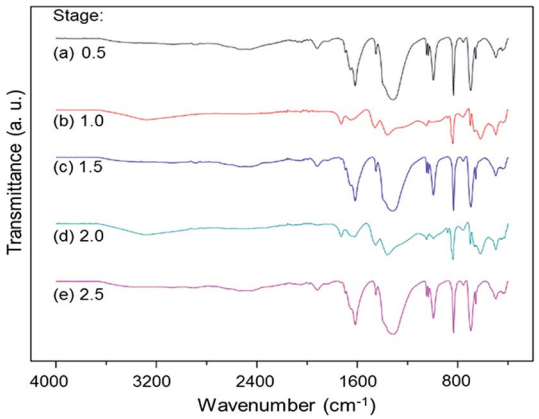

Fig. 9 ATR-FTIR spectra of Na_2ZrO_3 samples tested in carbonation–decarbonation stages.

Finally, sample spectrum treated in the stage 2.0 shows the presences of Na_2CO_3, as the only carbonated compound formed during the decomposition step under N_2 flow (stage 2.0); whereas a regeneration of $NaHCO_3$ was registered in the sample treated with CO_2 flow in the stage 2.5. This result confirms that it is possible to perform sequential carbonation–decarbonation processes over sodium zirconate and obtain a good regeneration of sodium bicarbonate and sodium carbonate after several decarbonation and carbonation steps at relatively low temperature.

In order to determinate the thermal behavior; products were characterized by thermogravimetric analyses (Fig. 10). Decomposition curves in Fig. 10A present two different behaviors. The profiles of samples treated in carbonated end-stages (0.5, 1.5 and 2.5) show higher weight decrease than samples treated in decarbonation end-stages (1.0 and 2.0). These results are in agreement with previous TG profiles presented in Fig. 5B and 8A. In samples treated in decarbonation end-stages, the weight lost is due to $NaHCO_3$ decomposition; whereas samples treated in decarbonation end-stages, exhibit a weight lost due to Na_2CO_3 dehydration. According to DTG profiles (Fig. 10B), decomposition processes take place at 127 and 115 °C, respectively. Also DTG profiles in Fig. 10B show that samples treated in carbonation end-stages, present the same decomposition temperature (127 °C) regardless the stage, however a decrease in the DTG curves was observed for the stages 1.5 and 2.5. A similar behavior was observed in the profiles of samples treated in decarbonation end-stages, where the same temperature was observed (115 °C) for this kind of stages.

Finally, a cyclability study was performed on this ceramic material in order to assess the regeneration properties after several cycles of carbonation and decarbonation. Fig. 11 shows the profiles obtained during eight carbonation and decarbonation processes. The maximum amount of CO_2 captured in the cycles 1–4 was higher than 64 wt% that is near to the amount chemisorbed in Fig. 5; whereas in the last four cycles, the amount of CO_2 captured decreases until 57.0 wt%. A decrease in the amount of CO_2 captured after eight cycles can be related to a decrement in the core shell formation due to the carbonation

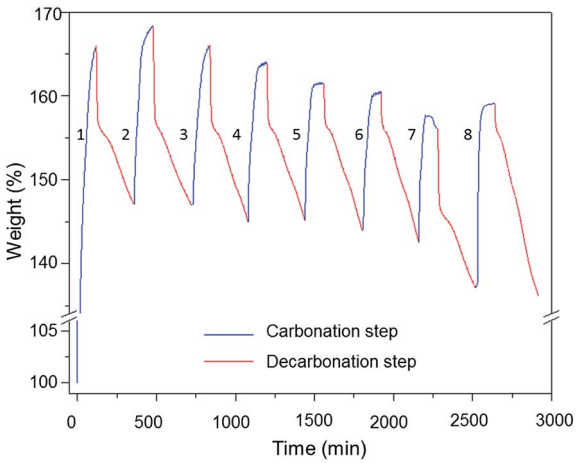

Fig. 11 Cyclability performance for CO_2 carbonation (2 h, 80 °C, 80% RH) and N_2 decarbonation (4 h, 80 °C, 40% RH).

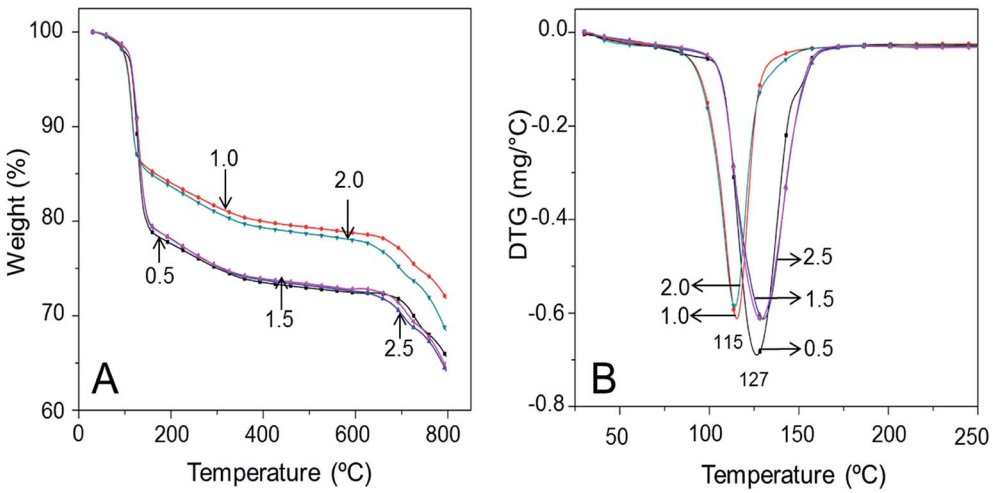

Fig. 10 TG (A) and DTG (B) curves of Na_2ZrO_3 samples tested in carbonation–decarbonation stages.

species chemisorbed. With the aim to determinate if the porous core shell was affected after cyclic tests, the product obtained was characterized by N_2 physisorption. As expected, the S_{BET} of the product was lower (6.9 $m^2\ g^{-1}$) than that reported for the sample treated dynamically (Fig. 3), but 2.3 times higher than the pristine material (3.0 $m^2\ g^{-1}$), indicating that after 8 cycles, the $NaHCO_3$ porous core shell still remains over the ceramic surface. The above results confirm that it is possible to accomplish successively carbonation–decarbonation steps at 80 °C, obtaining high regeneration of $NaHCO_3$ and Na_2CO_3 at the optimal values of relative humidity during carbonation (80% of RH) and decarbonation (40% of RH) processes.

4. Conclusions

In the present work, sodium zirconate was synthetized, characterized structurally and microstructural and also tested in carbonation step under CO_2 flow and decarbonation step under N_2 flow using different relative humidity conditions at 80 °C.

In carbonation process, the addition of water vapor into the reaction system significantly improves the CO_2 chemisorption. In fact, using low values of relative humidity, *e.g.* 10%, it was possible to capture 32.5 wt% of CO_2. This result is higher than the theoretical value calculated in dry conditions (23.8 wt%), and it was attributed to the $NaHCO_3$ formation. Also, in dynamic tests it was observed that when RH percentage increases, the CO_2 capture is significantly improved. Thus, at 80% of RH was the best condition for $NaHCO_3$ formation during carbonation step at 80 °C. At these physicochemical conditions, it was possible to capture the highest amount of CO_2, 13.0 mmol per gram of ceramic material. This amount is a high amount of CO_2 captured, considering the low temperature range employed.

Regarding to decarbonation process, it was observed a different behavior which depends strongly of the value of RH used. In this step three different cases were observed: (1) at RH < 20% it was observed the presence of Na_2O, which is a low stable compound, (2) at RH between 40 and 60%, only was detected the presence of sodium carbonate and (3) at RH = 80%, it was noticed the presence of small amounts Na_2CO_3 and also the presence of a high amounts of water condensed over the ceramic surface. Thus, the amount of Na_2CO_3 presented a maximum point at 40% of RH (DTG), which corresponds to the optimal condition for decarbonation step.

Finally, according to characterization results it can be established that using 80% of RH during carbonation step and 40% of RH in decarbonation step at 80 °C, it is possible to accomplish successively at least eight carbonation–decarbonation processes, obtaining high regeneration of sodium carbonates over the ceramic surface.

Acknowledgements

This work was financially supported by the project PAPIIT-UNAM (IN-101916). J. A. Mendoza-Nieto thanks DGAPA-UNAM for financial support. Authors thank to A. Tejeda for technical help.

References

1 S. Ma'mun, H. F. Svendsen, K. A. Hoff and O. Juliussen, *Energy Convers. Manage.*, 2007, **48**, 251–258.
2 T. F. Wall, *Proc. Combust. Inst.*, 2007, **31**, 31–47.
3 J. Gibbins and H. Chalmers, *Energy Policy*, 2008, **36**, 4317–4322.
4 D. M. D'Alessandro, B. Smit and J. R. Long, *Angew. Chem., Int. Ed.*, 2010, **49**, 6058–6082.
5 C. Lu, H. Bai, B. Wu, F. Su and J. F. Hwang, *Energy Fuels*, 2008, **22**, 3050–3056.
6 N. R. Stuckert and R. T. Yang, *Environ. Sci. Technol.*, 2011, **45**, 10257–10264.
7 J. R. Li, Y. Ma, M. C. McCarthy, J. Sculley, J. Yu, H. K. Jeong, P. B. Balbuena and H. C. Zhou, *Coord. Chem. Rev.*, 2011, **255**, 1791–1823.
8 A. Zárate, R. A. Peralta, P. A. Bayliss, R. Howie, M. Sánchez-Serratos, P. Carmona-Monroy, D. Solis-Ibarra, E. González-Zamora and I. A. Ibarra, *RSC Adv.*, 2016, **6**, 9978–9983.
9 X. Xu, C. Song, J. M. Andresen, B. G. Miller and A. W. Scaroni, *Energy Fuels*, 2002, **16**, 1463–1469.
10 C. Chen, W.-J. Son, K.-S. You, J.-W. Ahn and W.-S. Ahn, *Chem. Eng. J.*, 2010, **161**, 46–52.
11 S. Wang, S. Yan, X. Ma and J. Gong, *Energy Environ. Sci.*, 2011, **4**, 3805.
12 R. V. Siriwardane, C. Robinson, M. Shen and T. Simonyi, *Energy Fuels*, 2007, **21**, 2088–2097.
13 E. Ochoa-Fernández, M. Rønning, T. Grande and D. Chen, *Chem. Mater.*, 2006, **18**, 1383–1385.
14 S. M. Amorim, M. D. Domenico, T. L. P. Dantas, H. J. José and R. F. P. M. Moreira, *Chem. Eng. J.*, 2016, **283**, 388–396.
15 S. C. Lee, B. Y. Choi, C. K. Ryu, Y. S. Ahn, T. J. Lee and J. C. Kim, *Korean J. Chem. Eng.*, 2006, **23**, 374–379.
16 G. S. Grasa and J. C. Abanades, *Ind. Eng. Chem. Res.*, 2006, **45**, 8846–8851.
17 L. Li, X. Wen, X. Fu, F. Wang, N. Zhao, F. Xiao, W. Wei and Y. Sun, *Energy Fuels*, 2010, **24**, 5773–5780.
18 N. Santiago-Torres, I. C. Romero-Ibarra and H. Pfeiffer, *Fuel Process. Technol.*, 2014, **120**, 34–39.
19 J. A. Mendoza-Nieto, E. Vera and H. Pfeiffer, *Chem. Lett.*, 2016, **45**, 3–6.
20 B. Alcantar-Vázquez, E. Vera, F. Buitron-Cabrera, H. A. Lara-García and H. Pfeiffer, *Chem. Lett.*, 2015, **44**, 480–482.
21 D. Barraza Jiménez, M. A. Escobedo Bretado, D. Lardizábal Gutiérrez, J. M. Salinas Gutiérrez, A. López Ortiz and V. Collins-Martínez, *Int. J. Hydrogen Energy*, 2013, **38**, 2557–2564.
22 T. Zhao, E. Ochoa-Fernández, M. Rønning and D. Chen, *Chem. Mater.*, 2007, **19**, 3294–3301.
23 K. M. Ooi, S. P. Chai, A. R. Mohamed and M. Mohammadi, *Asia-Pac. J. Chem. Eng.*, 2015, 565–579.
24 I. Alcérreca-Corte, E. Fregoso-Israel and H. Pfeiffer, *J. Phys. Chem. C*, 2008, **112**, 6520–6525.
25 B. Alcántar-Vázquez, J. F. Gómez-García, G. Tavizon, I. A. Ibarra, C. Diaz, E. Lima and H. Pfeiffer, *J. Phys. Chem. C*, 2014, **118**, 26212–26218.

26 H. Pfeiffer, C. Vázquez, V. H. Lara and P. Bosch, *Chem. Mater.*, 2007, **19**, 922–926.
27 L. Martínez-dlCruz and H. Pfeiffer, *J. Phys. Chem. C*, 2012, **116**, 9675–9680.
28 G. G. Santillán-Reyes and H. Pfeiffer, *Int. J. Greenhouse Gas Control*, 2011, **5**, 1624–1629.
29 S. Kumar and S. K. Saxena, *Materials for Renewable and Sustainable Energy*, 2014, **3**, 1–15.
30 J. D. Figueroa, T. Fout, S. Plasynski, H. McIlvried and R. D. Srivastava, *Int. J. Greenhouse Gas Control*, 2008, **2**, 9–20.
31 J. Ortiz-Landeros, L. Martínez-Dlcruz, C. Gómez-Yáñez and H. Pfeiffer, *Thermochim. Acta*, 2011, **515**, 73–78.
32 L. Martínez-dlCruz and H. Pfeiffer, *J. Solid State Chem.*, 2013, **204**, 298–304.
33 A. López-Ortiz, N. G. P. Rivera, A. R. Rojas and D. L. Gutierrez, *Sep. Sci. Technol.*, 2005, **39**, 3559–3572.
34 P. Sánchez-Camacho, I. C. Romero-Ibarra, Y. Duan and H. Pfeiffer, *J. Phys. Chem. C*, 2014, **118**, 19822–19832.
35 S. Lowell, J. E. Shields, M. A. Thomas and M. Thommes, *Characterization of Porous Solids and Powders: Surface Area, Pore Size and Density*, Springer, Netherlands, Dordrecht, 2004, vol. 16.
36 S. C. Lee, H. J. Chae, S. J. Lee, B. Y. Choi, C. K. Yi, J. B. Lee, C. K. Ryu and J. C. Kim, *Environ. Sci. Technol.*, 2008, **42**, 2736–2741.
37 Y. Seo, S.-H. Jo, C. K. Ryu and C.-K. Yi, *Chemosphere*, 2007, **69**, 712–718.
38 G. Li, P. Xiao, P. Webley, J. Zhang, R. Singh and M. Marshall, *Adsorption*, 2008, **14**, 415–422.
39 T. Hatekeyama and L. Zhenhai, *Handbook of Thermal Analysis*, Wiley, 1998.
40 M. Hartman, O. Trnka and O. Šolcová, *Ind. Eng. Chem. Res.*, 2005, **44**, 6591–6598.
41 R. Rodríguez-Mosqueda and H. Pfeiffer, *Phys. Chem. C*, 2013, 2–11.
42 L. Martínez-Dlcruz and H. Pfeiffer, *J. Phys. Chem. C*, 2010, **114**, 9453–9458.
43 P. Sánchez-Camacho, I. C. Romero-Ibarra and H. Pfeiffer, *J. CO_2 Util.*, 2013, **3–4**, 14–20.